Effect of Electrolytes and Temperature on Dications and Radical Cations of Carotenoids: Electrochemical, Optical Absorption, and High-Performance Liquid Chromatography Studies

Zhangfei He and Lowell D. Kispert*

Department of Chemistry, The University of Alabama, Tuscaloosa, Alabama 35487

Received: June 10, 1999; In Final Form: September 29, 1999

The effect of supporting electrolytes and temperature on the behavior of dications and radical cations of carotenoids is studied. Cyclic voltammograms (CVs) of canthaxanthin (**I**) at 23 and −25 °C show that $Car^{\bullet+}$ of **I** has similar stability during the time of the CV scan, when using tetrabutylammonium perchlorate (TBAPC), tetrabutylammonium tetrafluoroborate (TBATFB), or tetrabutylammonium hexafluorophosphate (TBAHFP) as supporting electrolyte. However, the stability of Car^{2+} decreases when using TBAPC or TBATFB; β-carotene (**II**) shows similar behavior. The CV of **I** at −25 °C shows a strong cathodic wave (wave 6) near −0.15 V (vs Ag) with an intensity about half that of the neutral oxidation wave when TBAPC or TBATFB is the supporting electrolyte. When TBAHFP is used, wave 6 (ca. −0.05 V vs Ag) is ca. 8 times weaker than when TBAPC or TBATFB is used. This wave results from the reduction of a species that may be a decay product of Car^{2+} of **I**. Our results show that these electrolytes commonly used in electrochemical studies may affect the studied systems to different extents. In simultaneous bulk electrolysis (BE) and optical absorption spectroscopic measurements, the absorption band of Car^{2+} of **I** in the presence of 0.1 M TBAHFP can be observed by lowering the BE temperature to −20 °C. In the presence of 0.1 M TBAPC or TBATFB, this band is not observed, even at −50 °C. Isomerization of neutral **I** (as shown by HPLC and its blue absorption band shift) is observed only when the Car^{2+} absorption band is absent during BE. This observation, along with an increase of the neutral absorption band after stopping BE, suggests that the equilibrium $Car + Car^{2+} \rightleftharpoons 2Car^{\bullet+}$ is shifted to the left because Car^{2+} decays more quickly than $Car^{\bullet+}$ in the presence of electrolyte and this is a major path for formation of cis neutral species from cis $Car^{\bullet+}$. The optical absorption of Car^{2+} of **I** at 18 °C in the presence of 0.1 M TBAHFP is obtained, which suggests that Car^{2+} of **I** is not as unstable at room temperature in the presence of TBAHFP as was thought before.

Introduction

About 600 naturally occurring carotenoids have been isolated from plants, animals, and algae.[1] They play several essential roles in photosynthetic organisms.[2−4] One role is to serve as photoprotection agents by quenching (bacterio)chlorophyll ((B)chl) triplet states to prevent their reaction with molecular oxygen (which results in the formation of the damaging singlet oxygen) or directly reacting with singlet oxygen to detoxify it. Carotenoids can also protect photosynthetic organisms by dissipation of excess energy. Another role is to serve as light-harvesting antennae by absorbing light energy in the visible region of the spectrum, where (B)chls are not efficient absorbers, and then transferring energy for use in photochemical events. It has also been suggested that carotenoids may act as anticancer agents[5] probably because of their antioxidant and free radical quenching properties.[6,7]

The behavior of a variety of carotenoids in organic solvents has been studied by electrochemical, optical absorption spectroscopic, HPLC, EPR, and ENDOR (electron nuclear double resonance) methods.[8−13] The electrode and homogeneous reactions in Scheme 1 have been shown to take place in electrochemical processes of carotenoids.[8,9,14−17]

SCHEME 1

electrode reactions

$$Car \rightleftharpoons Car^{\bullet+} + e^- \quad (1)$$

$$Car^{\bullet+} \rightleftharpoons Car^{2+} + e^- \quad (2)$$

$$^{\#}Car^{\bullet} \rightleftharpoons {}^{\#}Car^{+} + e^- \quad (3)$$

homogeneous reactions

$$Car^{2+} + Car \rightleftharpoons 2Car^{\bullet+} \quad (4)$$

$$Car^{2+} \rightleftharpoons {}^{\#}Car^{+} + H^+ \quad (5)$$

$$Car^{\bullet+} \rightleftharpoons {}^{\#}Car^{\bullet} + H^+ \quad (6)$$

$^{\#}$Car represents the carotenoid with one less proton

For most carotenoids, the potential difference for forming radical cations ($Car^{\bullet+}$) and dications (Car^{2+}) (ΔE) is sufficiently large so that two anodic waves are observed in the cyclic voltammograms (CV). For some carotenoids, these potentials are nearly the same (for β-carotene, $\Delta E = 5$ mV).[9,16] Radical cations of carotenoids have been observed in photosynthetic reaction centers,[18−20] where they may play an important role in the electron-transfer processes. It is possible that Car^{2+} species are also formed and play a role in photosynthetic reaction centers. While $Car^{\bullet+}$ properties have been studied extensively,[10,21−24]

* To whom correspondence should be addressed.

10.1021/jp991904d CCC: $18.00
Published on Web 11/03/1999

little is known about those of Car^{2+}. The study of dications is important to better understand the roles and properties of carotenoids in photosynthetic organisms.

Supporting electrolytes have been shown to affect the electrochemical oxidation and reduction of some compounds.[25−29] For example, in the anodic oxidation of hexamethylbenzene,[25] the electroinactive anions of the supporting electrolytes (ClO_4^- and BF_4^-) have a pronounced effect on the product composition. When using tetrabutylammonium perchlorate (TBAPC) as supporting electrolyte in CH_3CN, the molar ratio of two major products, pentamethylbenzylacetamide (**A**) and pentamethylbenzyl acetate (**B**), is 78:22. When tetrabutylammonium tetrafluoroborate (TBATFB) is used as the supporting electrolyte, the molar ratio of product **A** to product **B** is 19:81. In the anodic oxidation of mesitylene, the product distribution also depends on the supporting electrolytes ($LiClO_4$, $NaClO_4$, TBAPC, TBATFB, and tetrabutylammonium hexafluorophosphate (TBAHFP)).[26] The rate of electron transfer in the electrochemical reduction of cyclooctatetraene depends largely on the size of the tetraalkylammonium cation:[27] the smaller the cation, the faster the reduction. In the electrochemical reduction of trans-15,16-dimethyldihydropyrene, the potential of the first cathodic wave was found to be independent of the supporting electrolyte; however, the second cathodic wave was at more negative potential when the cation of the supporting electrolyte was $(C_4H_9)_4N^+$ than when it was $(CH_3)_4N^+$.[28] This phenomenon was attributed to weaker ion pairing between the larger cation of the supporting electrolyte and the anion of the solute. Different halide supporting electrolytes (tetrabutylammonium as the cation) have been shown to have different effects on the redox properties of some meso-tetrasubstituted porphyrin free bases,[29] which were attributed to the different extent of interaction of halide ions with the porphyrin macrocycle. The interaction between halide ions and porphyrin can change the reduction pathways of the porphyrin. When the size of the halide ion was smaller, the interaction was larger, thus the reduction pathway of porphyrin was changed to a larger extent.

Recently, temperature has been shown to affect the electron-transfer rate in model systems for photosynthetic reaction centers (porphyrin−quinone dyads).[30] The rate constant of intramolecular photoinduced charge separation (CS) was shown to depend on temperature. Further, the activation energy of the CS process increased with a decrease of $-\Delta G_{cs}$. In contrast, the rate constant of intramolecular charge recombination (CR) was shown to be nearly independent of temperature, which means that in these systems the CR has little or no activation energy. Optical absorption spectra of carotenoids have been shown to be strongly dependent on temperature.[31] It is highly probable that temperature also affects the electron transfer between carotenoids and other molecules.

In this paper, we use electrochemistry, optical absorption spectroscopy, and HPLC to study the effect of supporting electrolytes and temperature on Car^{2+} and $Car^{\bullet+}$ of two carotenoids, canthaxanthin (**I**) and β-carotene (**II**); their structures are shown below.

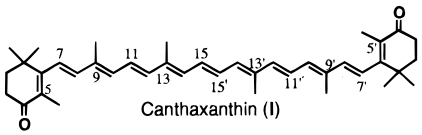

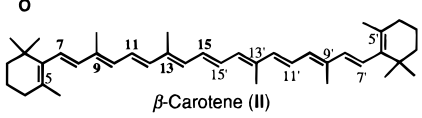

Experimental Section

All-trans canthaxanthin (**I**) and β-carotene (**II**) were obtained from Fluka. Both were stored over Drierite at −16 °C in containers that were wrapped with Parafilm and foil to avoid exposure to moisture and light. Prior to use, they were allowed to warm to room temperature. Anhydrous dichloromethane, purchased from Aldrich, was opened and kept in a drybox under a nitrogen atmosphere. All CH_2Cl_2 solutions of carotenoids were prepared in the drybox. Supporting electrolytes tetrabutylammonium hexafluorophosphate (TBAHFP), tetrabutylammonium perchlorate (TBAPC), and tetrabutylammonium tetrafluoroborate (TBATFB) were obtained from Fluka. According to the supplier, tetrabutylammonium bromide (TBABr) might be a trace impurity in these supporting electrolytes. In cyclic voltammetry of 0.1 M TBAHFP and 0.1 M TBAPC solutions, no wave corresponding to TBABr (oxidation potential: ca. 0.69 V vs SCE) appeared, which indicated that the concentration of TBABr in both solutions was lower than its detection limit (5 μM, glassy carbon with 3.0 mm diameter as the working electrode, CH_2Cl_2 as the solvent). The same method showed that the concentration of TBABr in 0.1 M TBATFB was $\leq$5 μM. The presence of 5 μM TBABr had no obvious effect on the CVs of carotenoids (1 mM in CH_2Cl_2). Recrystallized supporting electrolytes, two times (TBAPC) or three times (TBATFB) from an ethyl acetate−pentane mixture (both solvents were from Aldrich, anhydrous) and dried for 10 h under vacuum at 80 °C (TBAPC) or 23 °C (TBATFB), also showed no difference in our results. The supporting electrolytes were therefore used as received; as usual, care was taken to avoid exposure to moisture. All containers of supporting electrolytes were opened and kept in a drybox under a nitrogen atmosphere. Just before an experiment, ca. 400 mg (estimated by comparison to the volume of an accurately weighed sample) of supporting electrolyte was taken from the drybox. During the whole procedure, dry nitrogen was utilized to prevent exposure to moisture. Acetonitrile of HPLC grade, obtained from Fisher, was stirred with potassium carbonate for 24 h and sonicated for 20 min to remove any possible acid and dissolved gases. Anhydrous $FeCl_3$ was obtained from Sigma.

Cyclic voltammetry was carried out with the Bio Analytical System BAS-100W electrochemical analyzer. Except as noted, the working electrode was a glassy carbon disk (diameter 3.0 mm), the counter electrode was a platinum wire, and the pseudo reference electrode was a silver wire (SCE reference electrode cannot be used at temperatures lower than 0 °C). The solutions were purged with dry nitrogen to remove possible dissolved oxygen and kept under a nitrogen atmosphere. The cell was equipped with a jacket, through which methanol at a chosen temperature was continuously circulated. CV peak currents (I_p) were estimated following the method given by Bard and Faulkner.[32]

The electrochemical cell utilized in simultaneous bulk electrolysis (BE) and optical absorption measurements was described in ref 8. The optical path length of its quartz cuvette was 1 cm. The working electrode was a platinum gauze, the counter electrode was a platinum wire, and a silver wire was utilized as the pseudo reference electrode. The applied electrolysis potential was 1 V. UV−vis absorption spectra were recorded using a double-beam Shimadzu 1601 UVPC spectrophotometer. During measurement, the solution was stirred continuously. In measurements at temperatures below 23 °C, methanol at the chosen temperature was circulated through the cell holder and dry nitrogen was continuously passed over both

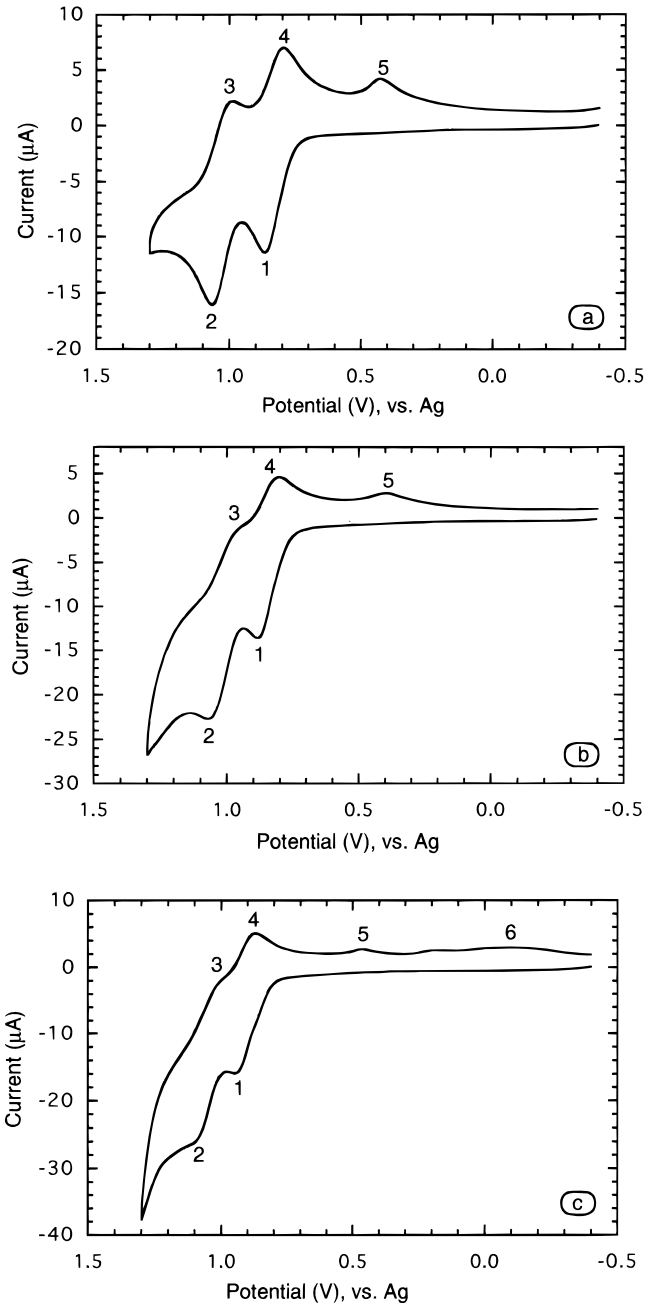

Figure 1. CVs of **I** in CH_2Cl_2 at 23 °C using 0.1 M different supporting electrolytes: (a) 0.7 mM **I** with TBAHFP; (b) 0.8 mM **I** with TBAPC; (c) 0.9 mM **I** with TBATFB. Scan rate is 0.1 V s^{-1}.

optical windows of the cuvette to prevent condensation of moisture.

HPLC separation was carried out at room temperature (23 °C) using a Shimadzu LC-600 pump equipped with a Rheodyne model 7125 injector, a PDA detector, and a Vydac 201 TP54 polymeric C18 column (250 mm × 4.6 mm i.d.) packed with 5 μm particles. The mobile phase was acetonitrile. Its flow rate was 1 mL min^{-1}. An amount of 10 μL of CH_2Cl_2 solution of carotenoids was injected each time.

AM1 (Austin model 1) semiempirical molecular orbital calculations[33] were carried out using HyperChem software on a Gateway 2000 P5-60 personal computer.

Results and Discussion

Cyclic Voltammetry. Figure 1 shows the cyclic voltammograms (CVs) of all-trans canthaxanthin (**I**) in CH_2Cl_2 containing

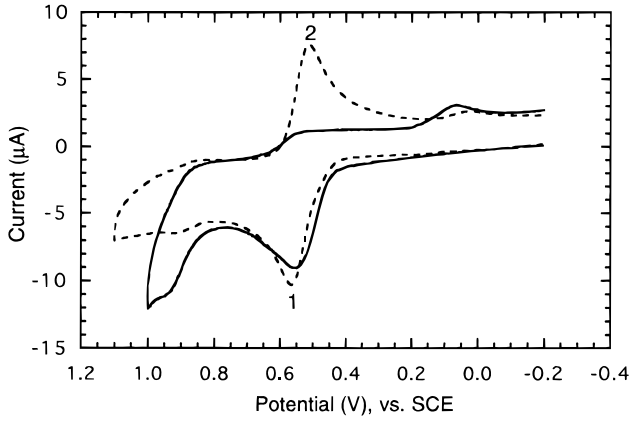

Figure 2. CVs of **II** in CH_2Cl_2 at 23 °C using 0.1 M different supporting electrolytes: (dotted line) 1.1 mM **II** with TBAHFP; (solid line) 1.0 mM **II** with TBATFB. Working electrode is Pt disk (diameter 1.6 mm), reference electrode is SCE, and counter electrode is Pt wire. Scan rate is 1 V s^{-1}.

0.1 M (a) TBAHFP, (b) TBAPC, (c) TBATFB as the supporting electrolyte at room temperature (23 °C) and a scan rate of 0.1 V s^{-1}. Anodic wave 1 is due to the one-electron oxidation of the neutral species, wave 2 to the one-electron oxidation of the resulting radical cation, and cathodic waves 3 and 4 correspond to the one-electron reductions of the dication and radical cation, respectively. Cathodic wave 5 is attributed to the reduction of $^{\#}Car^{+}$, which is derived from Car^{2+} by loss of one proton as shown in eq 5.[8,9,14−16] Comparison of the CVs measured in the presence of TBAHFP, TBAPC, and TBATFB showed no obvious intensity change in waves 1 and 2, and $I_{p1} \approx I_{p2}$ in all three cases. But the cathodic wave 3 decreased considerably when we utilized TBAPC or TBATFB instead of TBAHFP as the supporting electrolyte. In Figure 1a, I_{p3} is ca. 6.0 μA, whereas this wave is only a shoulder in parts b and c of Figure 1. The cathodic wave 4 also decreased. I_{p4}/C^* decreased by factors of ca. 1.3 and 1.5 when using TBAPC and TBATFB, respectively, where C^* is the bulk concentration of **I**. The decrease of wave 3 shows that the Car^{2+} of **I** is less stable when using TBAPC or TBATFB than when using THAHFP. The fact that no obvious intensity change of wave 2 (the oxidation of $Car^{\bullet+}$) occurred shows that the $Car^{\bullet+}$ of **I** has similar stability in the presence of these different supporting electrolytes. The reason for the decrease of wave 4 (the reduction of $Car^{\bullet+}$) is that fewer $Car^{\bullet+}$ species are generated in wave 3. In addition, the shape of the CVs changed. The effect of the electrolyte could even be observed at low concentration (ca. 1 mM) of TBAPC in 1 mM CH_2Cl_2 solution of **I** in the presence of 0.1 M TBAHFP. In this case, wave 3 decreased by a factor of ca. 1.1 compared to that without TBAPC.

When the scan rate was increased to 1 V s^{-1}, the decrease in intensities of waves 3 and 4 was still observed when using TBAPC or TBATFB instead of TBAHFP. Wave 3 was still only a shoulder, as in parts b and c of Figure 1, although it was somewhat more pronounced. I_p/C^* of wave 4 decreased by a factor of ca. 1.1 in both cases. When the scan rate was further increased to 10 V s^{-1}, the same CV of **I** was observed when using TBAHFP or TBAPC, but a very small decrease of wave 3 occurred when TBATFB was utilized. In short, the difference among CVs of **I** with different supporting electrolytes becomes smaller at higher scan rates. This dependence on the CV scan rate can be explained by less decay of Car^{2+} of **I** during the faster scans.

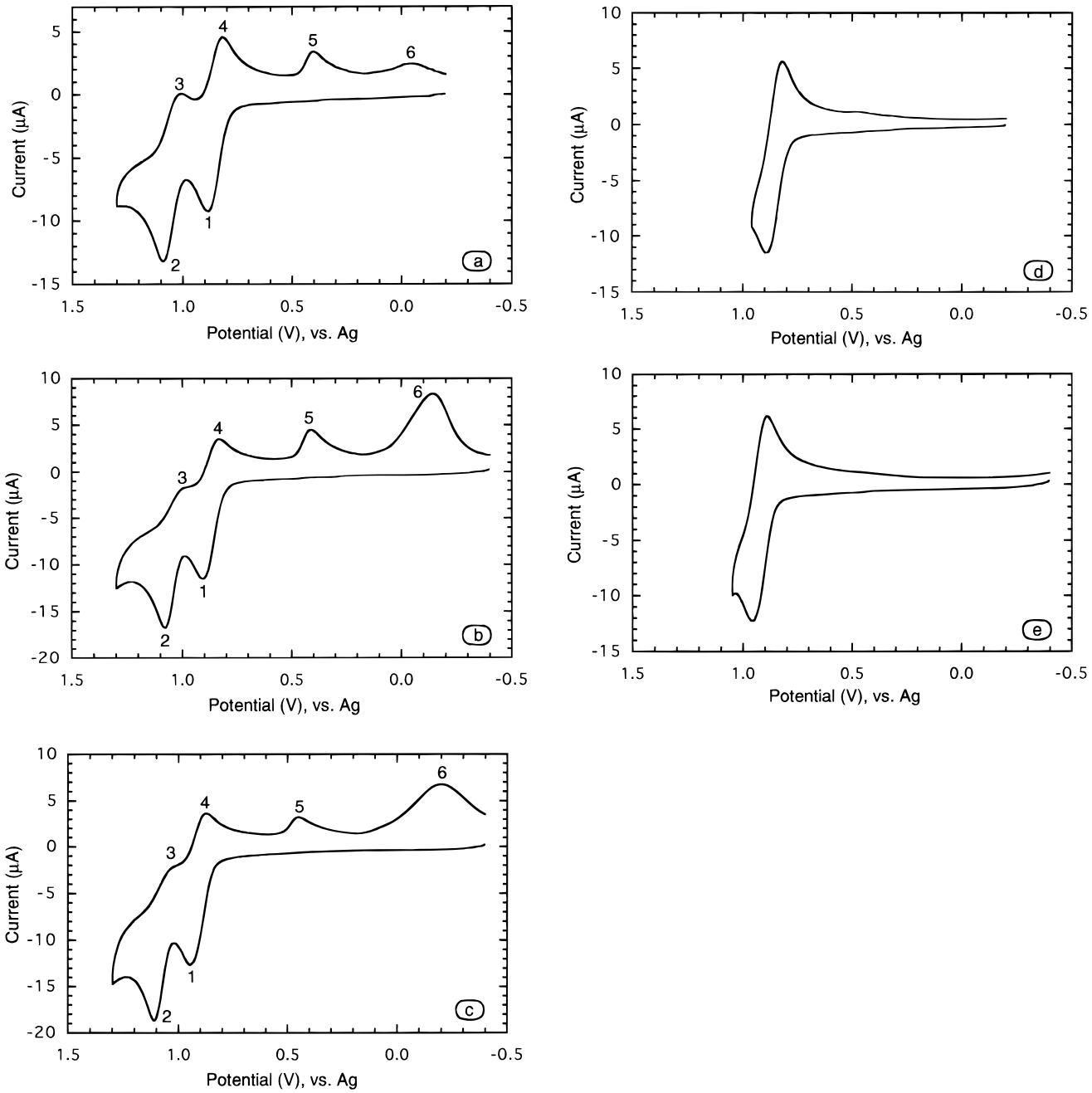

Figure 3. CVs of 0.9 mM **I** in CH_2Cl_2 at −25 °C using 0.1 M different supporting electrolytes: (a) with TBAHFP; (b) with TBAPC; (c) with TBATFB; (d) same condition as (b) except for scan reversal at lower potential; (e) same condition as (c) except for scan reversal at lower potential. Scan rate is 0.1 V s^{-1}.

In the study of β-carotene (**II**) at room temperature, a decrease of the cathodic wave also occurred when using TBAPC compared to that with TBAHFP (data not shown). At 0.1 V s^{-1} scan rate, I_p/C^* of the cathodic wave decreased by a factor of 4.0. Because the potentials of the one-electron reduction of Car^{2+} and the one-electron reduction of $Car^{\bullet+}$ of **II** are nearly the same ($E_2° - E_1° = 5$ mV), only one cathodic wave was observed.[14] (The same is true for the anodic process.) Since no obvious change occurred in the anodic wave when using different supporting electrolytes, we conclude that $Car^{\bullet+}$ of **II** has similar stability in both cases, but Car^{2+} is less stable in the presence of TBAPC than in the presence of TBAHFP, as in the case of **I**. Like **I**, when the scan rate was increased, the difference between the CVs using TBAPC and TBAHFP became smaller. At 1 V s^{-1} scan rate, I_p/C^* of the cathodic wave decreased by a factor of 2.7. At 10 V s^{-1} scan rate, it decreased by a factor of only 1.3.

When TBATFB was utilized, at scan rates less than 1 V s^{-1}, the cathodic wave of **II** was nearly undetectable (Figure 2 shows the CV at 1 V s^{-1}). Even when the scan rate reached 10 V s^{-1}, this cathodic wave was still weak (intensity ratio of cathodic wave to anodic wave $I_{pc}/I_{pa} = 0.16$).

Comparison of the CVs of **I** and **II** shows that the effect of supporting electrolytes is greater on **II** than on **I**.

All anions we studied have symmetric structures. The different effects of ClO_4^-, BF_4^-, and PF_6^- on the stability of Car^{2+} cannot be explained in terms of polarity. However, AM1 semiempirical molecular orbital calculations show that the energies of ClO_4^- and BF_4^- are higher than that of PF_6^- (Table 1). Further, the size of both ClO_4^- and BF_4^- is smaller than

TABLE 1: AM1 Energy Calculation (kcal mol^{-1}) of PF_6^-, ClO_4^-, and BF_4^-

	PF_6^-	ClO_4^-	BF_4^-
total energy	−70295.7	−37842.3	−46566.6
electronic energy	−205137.3	−89677.3	−104532.2

that of PF_6^-. Both energy and size factors are favorable for interaction of ClO_4^- and BF_4^- with Car^{2+}.

We also measured the CVs of **I** at −25 °C (Figure 3). At 0.1 V s^{-1} scan rate, unlike at room temperature, no pronounced change in the shapes of the CVs was observed when using TBAPC or TBATFB instead of TBAHFP as the supporting electrolyte. Nevertheless, the decrease of cathodic waves 3 and 4 was still observed, especially for wave 3; but the decreases were smaller than those at room temperature because of the slower decay of Car^{2+} at lower temperature. In parts b and c of Figure 3, wave 3 is still a shoulder and the I_p/C^* of wave 4 decreased by factors of 1.2 and 1.3 for TBAPC (Figure 3b) and TBATFB (Figure 3c), respectively, compared to the case using TBAHFP. As in Figure 1, the anodic waves 1 and 2 show no obvious intensity change in the three cases, and $I_{p1} \approx I_{p2}$. The CVs at −25 °C show similar effects of the supporting electrolytes on waves 1−4. The intensity of the cathodic wave 5 increased in all cases at lower temperature. I_{p5}/C^* increased by factors of 1.3, 3.4, and 2.7 for TBAHFP, TBAPC, and TBATFB, respectively, when the temperature was decreased from 23 to −25 °C, which indicates increasing stability of $^{\#}Car^+$ with decreasing temperature. The most notable phenomenon observed at −25 °C is the appearance of an additional cathodic wave (wave 6). When TBAHFP is used as the supporting electrolyte, wave 6 is weak (ca. 0.7 μA, −0.05 V vs Ag), whereas it is strong when TBAPC or TBATFB (6.6 and 5.5 μA, respectively, near −0.15 V vs Ag) is used at almost the same concentration of **I**. In the subsequent anodic scan, no obvious anodic wave corresponding to wave 6 was observed, which suggests that the species generated in wave 6 is extremely unstable. When the CV scan was reversed before Car^{2+} was formed, wave 6 was absent, as shown in parts d and e of Figure 3. Therefore, the species involved in wave 6 should be derived from Car^{2+}, not $Car^{\bullet+}$. Since the intensity of wave 5 is not very different when using different supporting electrolytes (I_p of wave 5 in parts a, b, and c of Figure 3 is 1.9, 3.1, and 1.9 μA, respectively), wave 6 is not due to the reduction of $^{\#}Car^{\bullet}$, which is generated in wave 5. In addition, $^{\#}Car^{\bullet}$ can also be generated from $Car^{\bullet+}$ (eq 6). Wave 6 should be due to a decay product of Car^{2+} other than $^{\#}Car^+$ (eq 5). ClO_4^- and BF_4^- can cause faster decay of Car^{2+} than PF_6^-, which is in accord with the decrease of the Car^{2+} reduction wave when using TBAPC or TBATFB instead of TBAHFP as the supporting electrolyte.

Comparison of parts d and b, and parts e and c of Figure 3 shows that the reduction wave of $Car^{\bullet+}$ increases ($I_{pa} \approx I_{pc}$) in parts d and e of Figure 3. This is further evidence for our conclusion that the decrease of wave 4 in previous CVs (Figures 1b,c and 3b,c) is due to the generation of fewer radical cations in wave 3.

At room temperature, wave 6 was not observed, although a very small (ca. 0.3 μA), broad wave 6 was present when TBATFB was used (Figure 1c). The absence of wave 6 at room temperature is attributable to the high instability of this decay product. Lowering the temperature increases its stability.

HPLC and Simultaneous Electrolysis and Optical Absorption Spectroscopic Measurements. Parts A, B, and C of Figure 4 show the changes of optical absorption spectra of neutral **I** during bulk electrolysis (BE) at room temperature using

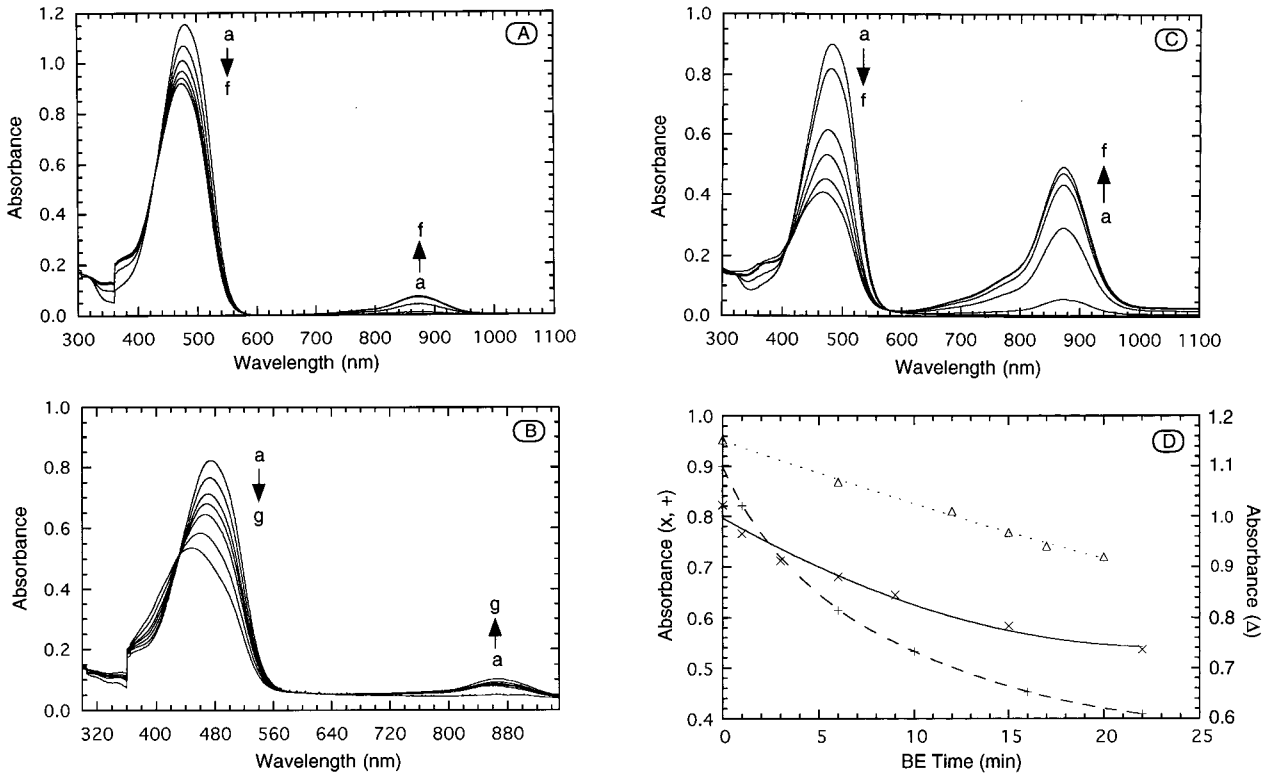

Figure 4. (A−C) Change of optical absorption spectra of **I** during BE at 1 V (23 °C). Initial concentrations of **I** are (A) 9.9 μM, (B) 7.0 μM, and (C) 7.7 μM with 0.1 M (A) TBATFB, (B) TBAPC, and (C) TBAHFP as supporting electrolyte. (A) BE for (a) 0, (b) 6, (c) 12, (d) 15, (e) 17, and (f) 20 min. (B) BE for (a) 0, (b) 1, (c) 3, (d) 6, (e) 9, (f) 15, and (g) 22 min. (C) BE for (a) 0, (b) 1, (c) 6, (d) 10, (e) 16, and (f) 22 min. Before BE, the absorption of neutral **I** (all-trans) is at 481 nm. The absorption of $Car^{\bullet+}$ is at (A) 872 nm, (B) 881 nm, and (C) 877 nm. (D) Decrease of optical absorbance of neutral **I** is shown with increasing periods of BE with 0.1 M (···) TBATFB, (−) TBAPC, (- - -) TBAHFP. Data are from parts A−C.

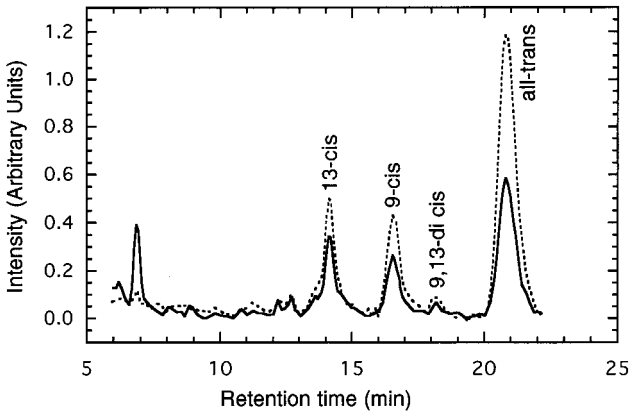

Figure 5. HPLC after BE of 5.4 μM **I** for 5 min (1 V, 23 °C). Supporting electrolyte is 0.1 M TBAHFP. Detector wavelengths are (−) 420 nm and (···) 481 nm.

TBATFB, TBAPC, and TBAHFP as the supporting electrolyte, respectively. Figure 4D shows the absorbance changes of neutral **I** (data from parts A−C of Figure 4). With TBATFB or TBAPC, the BE rate was smaller than with TBAHFP under the same experimental conditions. After 6 min of BE, 7%, 17%, and 32% of neutral **I** was electrolyzed when using TBATFB, TBAPC and TBAHFP, respectively. At −25 °C, the behavior was similar. During BE at room temperature, using TBATFB or TBAPC, a low-intensity absorption band of $Car^{\bullet+}$ appeared and a blue shift of the neutral absorption band occurred (parts A and B of Figure 4). In Figure 4A, curves a−f, there is a 6 nm blue shift; in Figure 4B, curves a−g, there is a 26 nm blue shift. During BE at room temperature and using TBAHFP, much more $Car^{\bullet+}$ appeared (Figure 4C) than when using TBAPC or TBATFB. Its concentration increased by a factor of ca. 7.0. The blue shift of the neutral absorption band was also observed (Figure 4C, curves a−f, 15 nm blue shift). At room temperature and similar concentrations of both the neutral and $Car^{\bullet+}$ species of **I**, the half-life time of $Car^{\bullet+}$ of **I** in CH_2Cl_2 was shortened by a factor of ca. 2.0 and 2.5 when using TBAPC and TBATFB, respectively, compared to that using TBAHFP. This result is different from that in the CVs, which did not indicate any obvious stability change of $Car^{\bullet+}$ of **I** when using different supporting electrolytes. This will be discussed later in this section. At −25 °C, 7 times as much $Car^{\bullet+}$ of **I** (maximum concentration) appeared during BE than at room temperature when using TBAPC. In the presence of TBAHFP, the maximum concentration of $Car^{\bullet+}$ of **I** increased by a factor of 4.0 when the temperature was changed from 23 to −25 °C. Although lowering the temperature increases the $Car^{\bullet+}$ stability, there was still only ca. $^1/_5$ as much $Car^{\bullet+}$ (maximum concentration) when using TBAPC than when using TBAHFP. Further, at −25 °C, the blue absorption band shift of the neutral species of **I** did not occur when using TBAHFP.

The blue band shift of the neutral species of **I** may be due to partial geometrical isomerization during BE.[31] Previous work in our group showed that geometrical isomerization of carotenoids can occur via their $Car^{\bullet+}$ or Car^{2+} species generated by BE or $FeCl_3$ oxidation.[11,34] All-trans $Car^{\bullet+}$ and Car^{2+} can change their conformation to cis structures more easily than the neutral species. The various conformational isomers are then converted to the neutral species. Figure 5 shows the HPLC results after BE (TBAHFP, CH_2Cl_2) of pure all-trans **I** at room temperature. After BE for 5 min, in addition to the all-trans neutral species, several isomers (9-cis, 13-cis, 9,13-di-cis)[11,34] appeared. If BE is stopped after 56% of all-trans neutral **I** has been electrolyzed (TBAHFP), subsequent optical absorption measurements of the

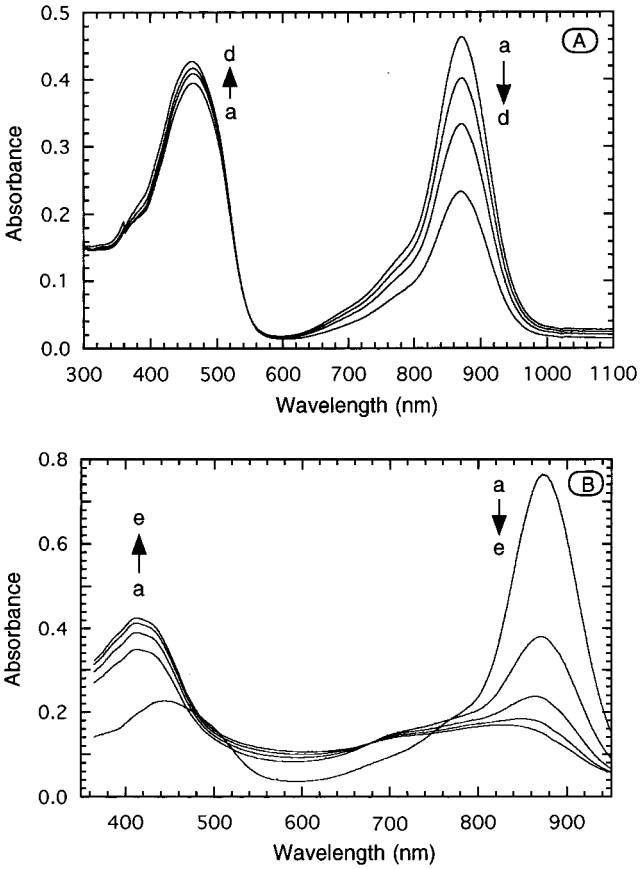

Figure 6. Change of optical absorption spectra of **I** with increasing periods of time after stopping BE (1 V, 23 °C). The solution was sealed and stirred continuously. Supporting electrolyte is 0.1 M TBAHFP. (A) Initial concentration of **I** is 7.7 μM, using a cell with a less porous frit at (a) 0, (b) 2, (c) 5, and (d) 13 min after stopping BE. (B) Initial concentration of **I** is 6.3 μM, using a cell with a more porous frit to obtain more extensive electrolysis at (a) 0, (b) 2, (c) 3, (d) 4, and (e) 5 min after stopping BE.

stirred solution showed a decrease of $Car^{\bullet+}$ and an increase and further small blue band shift of the neutral species (Figure 6A, from 464 nm (a) to 461 nm (d)). Since the increase in intensity and the further blue band shift of the neutral species are small, whereas the decrease of $Car^{\bullet+}$ absorption is large, there must be more than one reaction of $Car^{\bullet+}$, and only one (or several) of which leads to the neutral species. When the amount of $Car^{\bullet+}$ generated by $FeCl_3$ oxidation at room temperature was similar to that generated in BE (and the amount of remaining neutral species was also similar to that in BE), no increase of the neutral species absorption was observed and the $Car^{\bullet+}$ absorption decreased slowly. We could not generate sufficient amounts of $Car^{\bullet+}$ of **I** in the presence of TBATFB or TBAPC to establish whether a similar phenomenon occurs. But from the slower BE rates (as determined by the decrease in absorption of **I**) than when using TBAHFP (see Figure 4), it is possible that more $Car^{\bullet+}$ was reconverted to the neutral species.

Another compound, with short HPLC retention time (6.87 min, Figure 5, solid line) and maximum absorption at 420 nm, was also formed during BE. If the PDA detector is set at 481 nm (absorption maximum of all-trans neutral **I**), this species is scarcely detectable in HPLC (Figure 5, dotted line). When a more porous frit was used to allow faster electrolysis (TBAHFP, CH_2Cl_2, room temperature), 75% of all-trans neutral **I** was consumed in 3 min. During BE, the large blue shift of the neutral species from 481 nm (before BE) to 443 nm (after 3 min BE) occurred. After stopping BE, aside from the faster decrease of

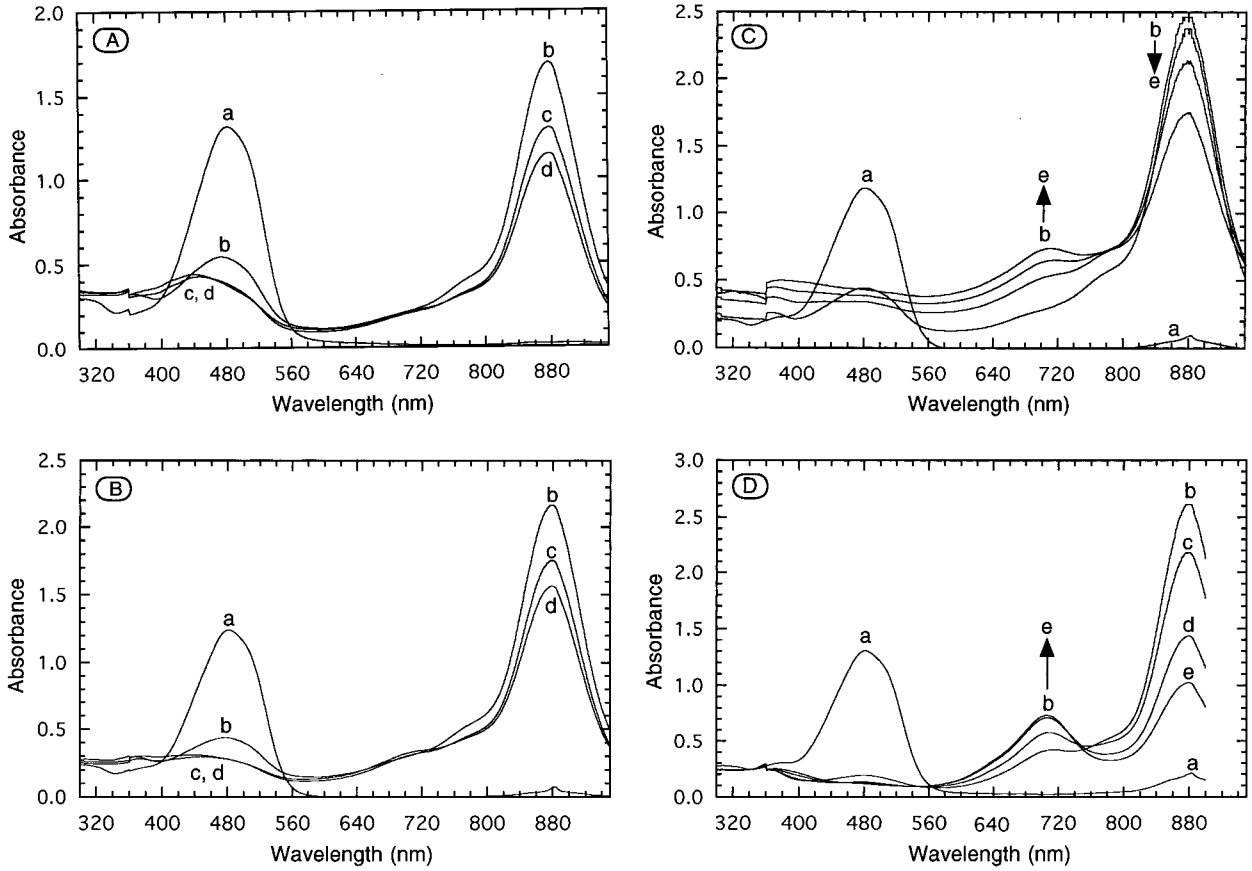

Figure 7. Change of optical absorption spectra of **I** with increasing periods of BE (1 V) at various temperatures. Supporting electrolyte is 0.1 M TBAHFP. (A) The temperature is −0.7 °C, and the initial concentration of **I** is 11.3 μM. BE for (a) initial (481 nm), (b) 30 (474 nm), (c) 62 (446 nm), and (d) 74 min. (B) The temperature is −10 °C, and the initial concentration of **I** is 10.6 μM. BE for (a) initial (481 nm), (b) 42 (476 nm), (c) 86, and (d) 104 min. (C) The temperature is −20 °C, and the initial concentration of **I** is 10.3 μM. BE for (a) initial (481 nm), (b) 32 (480 nm), (c) 74, (d) 102, and (e) 142 min. (D) The temperature is −25 °C, and the initial concentration of **I** is 11.2 μM. BE for (a) initial (481 nm), (b) 50 (481 nm), (c) 72, (d) 106, and (e) 136 min. Values in parentheses are the wavelengths at the absorption maxima of neutral species of **I**. The absorption band at 709 nm is due to Car^{2+} of **I**.

$Car^{\bullet+}$ absorption than when using the less porous frit (Figure 6A), an absorption band appeared and increased at ca. 420 nm (Figure 6B). Comparison of parts A and B of Figure 6 shows that the main decay product(s) and decay rate of $Car^{\bullet+}$ of **I** depend on the ratio of $Car^{\bullet+}$ to the neutral species in the solution.

At room temperature, the optical absorption band of Car^{2+} (714 nm) of **I** can be observed by chemically oxidizing the neutral species with $FeCl_3$.[35] This band cannot be observed during BE at room temperature, even when using TBAHFP as the supporting electrolyte. The reason is that, unlike $FeCl_3$ oxidation, BE is a slow process and Car^{2+} is not as stable as $Car^{\bullet+}$. However, as the temperature is decreased, the Car^{2+} absorption band becomes more and more evident during BE using TBAHFP (Figure 7). At −20 °C, this band is an obvious peak at 709 nm. At −25 °C, this peak becomes stronger. After BE at −25 °C for 100 min, 5 times as much Car^{2+} was present than at −20 °C during the same time. During BE with TBAPC or TBATFB, the absorption of Car^{2+} of **I** was not observed, even at −50 °C; but the blue absorption band shift of neutral **I** occurred. Under the same experimental conditions as in parts A and B of Figure 4, except at −50 °C, there is a 15 nm blue shift after 120 min BE when using TBAPC, and a 7 nm blue shift after 140 min BE when using TBATFB.

An interesting phenomenon is that when the Car^{2+} absorption band is observed during BE, no absorption band shift of the neutral species occurs; but when the Car^{2+} absorption band is absent, the absorption band shift of the neutral species occurs (see figure caption of Figure 7 for the wavelengths at the absorption maxima). This and other phenomena suggest that the equilibrium in eq 4 can be easily driven to the left in the presence of excess electrolyte, especially TBATFB or TBAPC, as a result of rapid decay of Car^{2+} induced by these electrolytes.

We briefly summarize relevant phenomena and explanations as follows. (1) After stopping BE at 23 °C, the amount of $Car^{\bullet+}$ of **I** decreased; at the same time, that of the neutral species of **I** increased (Figure 6A), whereas no similar phenomenon was observed in the $FeCl_3$ oxidation. Because Car^{2+} decays faster than $Car^{\bullet+}$ in the presence of electrolyte, the equilibrium in eq 4 is driven to the left and thus the neutral species increases. (2) At lower temperatures, Car^{2+} is sufficiently stable to permit observation of its absorption during BE; no blue shift of the neutral species occurs (Figure 7). In BE, isomerization of the neutral species may occur via $Car^{\bullet+}$. As Car^{2+} becomes more stable at lower temperature, less cis $Car^{\bullet+}$ will become the cis neutral species through the shift of equilibrium in eq 4. Thus, less isomerization occurs. From this phenomenon, we can further deduce that the left shift of equilibrium in eq 4 is a major path by which the cis $Car^{\bullet+}$ becomes the cis neutral species. (3) BE was slower when using TBATFB or TBAPC than when using TBAHFP as the supporting electrolyte (Figure 4). Because TBATFB and TBAPC destabilized Car^{2+} to a greater extent than TBAHFP (see CV results), more $Car^{\bullet+}$ was converted to the neutral species through the equilibrium in eq 4. BE thus appeared to be slower, and fewer $Car^{\bullet+}$ species were detected. The half-life time of $Car^{\bullet+}$ in the presence of TBATFB or TBAPC was also shortened. This apparent stability decrease of

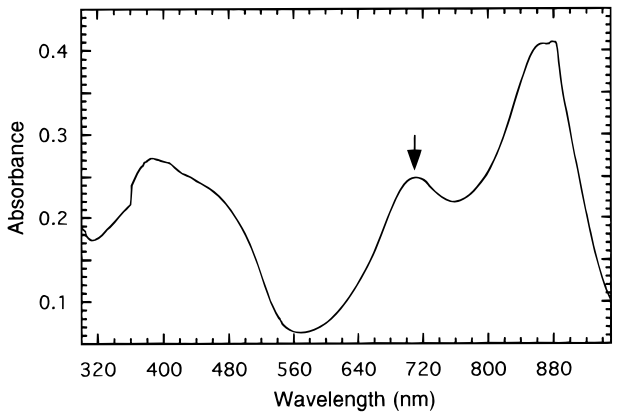

Figure 8. Optical absorption spectrum of Car^{2+} of **I** at 18 °C in the presence of 0.1 M TBAHFP generated by electrolyzing 11.8 μM **I** for 150 min at 1 V, −25 °C, then stopping BE and allowing the temperature to increase to 18 °C (in 40 min).

$Car^{\bullet+}$ in BE in the presence of TBATFB or TBAPC (compared to TBAHFP) is essentially due to the stability decrease of Car^{2+}. Because a CV scan is fast (only ca. 2 s for scanning from wave 1 to wave 2 when the scan rate is 0.1 V s^{-1}), the slow reverse reaction of the equilibrium in eq 4 (as shown in Figure 6) has no obvious effect on wave 2 in the CVs.

To further assess the stability of Car^{2+} in the presence of 0.1 M TBAHFP at room temperature, we generated Car^{2+} of **I** by BE at −25 °C, then allowed the temperature to increase. When the temperature had increased to 18 °C (in 40 min), the optical absorption band of Car^{2+} of **I** was still evident (Figure 8). Once generated, Car^{2+} can exist for ca. 10 min at 18 °C before it totally disappears. This result suggests that Car^{2+} of **I** is not as unstable at room temperature in the presence of 0.1 M TBAHFP as had been concluded before.[35] The reason for the failure to observe Car^{2+} during BE at room temperature is the length of time it takes to perform BE. During a CV, however, the scan rate is much faster and sufficient Car^{2+} survives at room temperature to observe a pronounced reduction wave of Car^{2+} when TBAHFP is utilized as the supporting electrolyte (Figure 1a, 0.1 V s^{-1} scan rate). In Figure 1a, I_{pc}/I_{pa} for Car^{2+} (wave 3/wave 2) is ca. 0.6.

Conclusions

Dications of carotenoids are less stable in the presence of 0.1 M TBAPC or TBATFB than in the presence of 0.1 M TBAHFP. Whereas the radical cations per se of carotenoids have similar stability in the three cases, their observed lifetime can be indirectly affected through the shift of the equilibrium Car + $Car^{2+} \rightleftharpoons 2Car^{\bullet+}$. Although all three supporting electrolytes are commonly used in electrochemical experiments, they may affect the studied systems to different extents. TBAHFP is the best choice in the study of carotenoids. Car^{2+} of **I** at room temperature in the presence of TBAHFP is not as unstable as was concluded before. Its optical absorption band at 18 °C is observed, which suggests that Car^{2+} may also be involved in photosynthetic reaction centers. A previously undetected decay product of Car^{2+} can be clearly observed in a CV but only at lower temperature (−25 °C in our experiment). The left shift of equilibrium Car + $Car^{2+} \rightleftharpoons 2Car^{\bullet+}$, due to the lower stability of Car^{2+} than $Car^{\bullet+}$ in the presence of electrolyte, is shown to be a major path for the formation of cis neutral species from cis $Car^{\bullet+}$. Isomerization of the neutral all-trans carotenoids is indicated by a blue absorption band shift and HPLC analysis.

Acknowledgment. We thank Drs. Elli S. Hand, Guoqiang Gao, and Dezhong Liu for helpful discussions. This work is supported by the Division of Chemical Science, Office of Basic Energy Sciences, Office of Energy Research, U.S. Department of Energy under Grant No. DE-FG02-86-ER13465.

References and Notes

(1) Straub, O. In *Key to Carotenoids*; Pfander, H. P., Ed.; Birkhäuser Verlag: Basel, 1987.
(2) Goedheer, J. C. *Annu. Rev. Plant Physiol*. **1972**, *23*, 87.
(3) Koyama, Y. *J. Photochem. Photobiol*. **1991**, *139*, 265.
(4) Frank, H. A.; Cogdell, R. J. *Photochem. Photobiol*. **1996**, *63*, 257.
(5) Ziegler, R. G. *Am. J. Clin. Nutr*. **1991**, *53*, 2515.
(6) Burton, G. W.; Ingold, K. U. *Science* **1984**, *224*, 569.
(7) Krinsky, N. I. *Clin. Nutr*. **1988**, *7*, 107.
(8) Grant, J. L.; Kramer, V. J.; Ding, R.; Kispert, L. D. *J. Am. Chem. Soc*. **1988**, *110*, 2151.
(9) Jeevarajan, J. A.; Kispert, L. D. *J. Electroanal. Chem.* **1996**, *411*, 57.
(10) Piekara-Sady, L.; Jeevarajan, A. S.; Kispert, L. D. *Chem. Phys. Lett.* **1993**, *207*, 173.
(11) Wei, C. C.; Gao, G.; Kispert, L. D. *J. Chem. Soc., Perkin Trans.* **1997**, *2*, 783.
(12) Gao, G.; Deng, Y.; Kispert, L. D. *J. Phys. Chem*. *B* **1997**, *101*, 7844.
(13) Khaled, M.; Hadjipetrou, A.; Kispert, L. D. *J. Phys. Chem.* **1990**, *94*, 5164.
(14) Mairanovsky, V. G.; Engovatov, A. A.; Ioffe, N. T.; Samokhvalov, G. I. *J. Electroanal. Chem.* **1975**, *66*, 123.
(15) Khaled, M.; Hadjipetrou, A.; Kispert, L. D.; Allendoerfer, R. D. *J. Phys. Chem.* **1991**, *95*, 2438.
(16) Jeevarajan, A. S.; Khaled, M.; Kispert, L. D. *J. Phys. Chem.* **1994**, *98*, 7777.
(17) Jeevarajan, A. S.; Khaled, M.; Kispert, L. D. *Chem. Phys. Lett.* **1994**, *225*, 340.
(18) Mathis, P.; Vermeglio, A. *Biochim. Biophys. Acta* **1975**, *396*, 371.
(19) Mathis, P.; Rutherford, A. W. *Biochim. Biophys. Acta* **1984**, *767*, 217.
(20) Telfer, A.; De Las Rivas, J.; Barber, J. *Biochim. Biophys. Acta* **1991**, *1060*, 106.
(21) Land, E. J.; Lexa, D.; Bensasson, R. V.; Gust, D.; Moore, T. A.; Moore, A. L.; Liddell, P. A.; Nemeth, G. A. *J. Phys. Chem.* **1987**, *91*, 4831.
(22) Jeevarajan, A. S.; Kispert, L. D.; Piekara-Sady, L. *Chem. Phys. Lett.* **1993**, *209*, 269.
(23) Edge, R.; Land, E. J.; McGarvey, D.; Mulroy, L.; Truscott, T. G. *J. Am. Chem. Soc*. **1998**, *120*, 4087.
(24) Tinkler, J. H.; Tavender, S. M.; Parker, A. W.; McGarvey, D. J.; Mulroy, L.; Truscott, T. G. *J. Am. Chem. Soc.* **1996**, *118*, 1756.
(25) Nyberg, K. *Chem. Commun.* **1969**, 774.
(26) Nyberg, K. *Acta Chem. Scand.* **1971**, *25*, 534.
(27) Fry, A. J.; Hutchins, C. S.; Chung, L. L. *J. Am. Chem. Soc.* **1975**, *97*, 591.
(28) Fry, A. J.; Chung, L. L.; Boekelheide, V. *Tetrahedron Lett.* **1974**, *5*, 445.
(29) Brett, C. M. A.; Oliveira Brett, A. M. C. F. *J. Electroanal. Chem.* **1988**, *255*, 199.
(30) Asahi, T.; Ohkohchi, M.; Matsusaka, R.; Mataga, N.; Zhang, R. P.; Osuka, A.; Maruyama, K. *J. Am. Chem. Soc*. **1993**, *115*, 5665.
(31) Britton, G. In *Carotenoids*; Britton, G., Liaaen-Jensen, S., Pfander, H., Eds.; Birkhäuser Verlag: Basel, 1995; Vol. 1B.
(32) Bard, A. J.; Faulkner, L. R. *Electrochemical Methods, Fundamentals and Applications*; John Wiley & Sons: New York, 1980.
(33) Dewar, M. J. S.; Zoebisch, E. G.; Healy, E. F.; Stewart, J. J. P. *J. Am. Chem. Soc.* **1985**, *107*, 3902.
(34) Gao, G.; Wei, C. C.; Jeevarajan, A. S.; Kispert, L. D. *J. Phys. Chem.* **1996**, *100*, 5362.
(35) Jeevarajan, J. A.; Wei, C. C.; Jeevarajan, A. S.; Kispert, L. D. *J. Phys. Chem.* **1996**, *100*, 5637.